



# A test method for measuring chloride diffusion coefficients through nonsaturated concrete

## Part I. The instantaneous plane source diffusion case

Miguel A. Climent<sup>a,\*</sup>, Guillem de Vera<sup>a</sup>, Jesús F. López<sup>a</sup>, Estanislao Viqueira<sup>b</sup>, Carmen Andrade<sup>c</sup>

<sup>a</sup>*Departament d'Enginyeria de la Construcció, Obres Públiques i Infraestructura Urbana, Universitat d'Alacant, Apartado Correos 99, 03080 Alicante, Spain*

<sup>b</sup>*Consultores Técnicos de la Construcción S.L. (Consulteco), Pol. Ind. Pla de la Vallonga, calle 6, Alicante, Spain*

<sup>c</sup>*Instituto de Ciencias de la Construcción Eduardo Torroja, CSIC, C/Serrano Galvache s/n, 28033 Madrid, Spain*

Received 3 January 2001; received in revised form 24 January 2002

### Abstract

A test method is proposed for measuring chloride diffusion coefficients through nonsaturated concrete specimens with controlled water contents. The experimental setup used allows one to supply an initial limited amount of  $\text{Cl}^-$  to the tested concrete surface. The procedure consists of submitting the surface of concrete specimens to interaction with the products of combustion of PVC, which contain mainly gaseous hydrogen chloride. This interaction yields a limited  $\text{Cl}^-$  contamination of the concrete surface. After returning the specimens to their controlled humidity exposure conditions, the kinetics of  $\text{Cl}^-$  transport from the surface inwards may be studied. The experimental  $\text{Cl}^-$  concentration profiles determined at selected time intervals have been adjusted to a diffusion model of “instantaneous plane source,” which takes into account the particular initial and boundary conditions of the experimental procedure, for obtaining the corresponding diffusion coefficients. © 2002 Published by Elsevier Science Ltd.

**Keywords:** Chloride; Diffusion; Concrete; Humidity; Modeling

### 1. Introduction

Chloride ingress and transport through concrete is an interesting technical and scientific subject of study and discussion due both to the reinforcement corrosion promoter character of  $\text{Cl}^-$  ions and to the complexity of the physical–chemical interactions among saline solutions, solid phases of concrete, and moisture.

Different and simultaneous mechanisms of  $\text{Cl}^-$  ingress and transport may operate due to the different environmental conditions to which a concrete structure may be exposed in a saline environment. Pure diffusion seems to operate only in water-saturated concrete, for instance, in the case of sea immersed structures. For the case of concrete exposed to marine atmospheres or deicing salts, the cyclic wetting and drying coupled with the effect of winds induce a nonsaturated state of concrete and an inhomogeneous spa-

tial distribution of moisture within concrete. In these conditions, both capillary sorption and diffusion may contribute to  $\text{Cl}^-$  transport.

The importance of the moisture state of concrete on the rate of ionic transport has been recognized [1], but it has been impossible, up to our knowledge, to determine experimentally the  $\text{Cl}^-$  diffusion coefficient in nonsaturated conditions. This fact may be explained by the need of maintaining a controlled and homogeneously distributed water content of concrete during the tests, which is incompatible, for instance, with natural diffusion experiments, i.e., ponding tests, in which the concrete surface is in contact with a  $\text{Cl}^-$  solution.

The objective of this work is to study and measure the diffusivity of  $\text{Cl}^-$  ions through nonsaturated concrete by means of an innovative testing methodology. The experimental technique allows studying the influence of the degree of water saturation of concrete upon  $\text{Cl}^-$  diffusion, avoiding contributions of other different mechanisms of  $\text{Cl}^-$  transport. To this end, samples with controlled water contents have been used, and an experimental setup has

\* Corresponding author. Tel.: +34-96-590-3707; fax: +34-96-590-3678.  
E-mail address: ma.climent@ua.es (M.A. Climent).

been developed to allow one to supply an initial limited amount of  $\text{Cl}^-$  to the tested concrete surface, without disturbing the water content of the concrete. The procedure consists of submitting the surface of the concrete specimens to interaction with the products of combustion of PVC [2], which contain mainly gaseous hydrogen chloride. After returning the specimens to their controlled humidity exposure conditions, the kinetics of  $\text{Cl}^-$  diffusion from the surface inwards may be studied. The experimental  $\text{Cl}^-$  concentration profiles determined at selected time intervals have been adjusted to a particular solution of Fick's second law of diffusion that corresponds to the case of an "instantaneous plane source" [3] (to obtain the corresponding diffusion coefficients, see Appendix A). The binding of  $\text{Cl}^-$  ions has not been considered for the model used in this part of the work.

Regarding the expected relationship between the  $\text{Cl}^-$  diffusion coefficient and the degree of water saturation of concrete, it must be taken into account that ionic species are brought by or move through the liquid phase that exists within the concrete pore network. If the transport of water is prevented and in the absence of other force fields,  $\text{Cl}^-$  ions can only diffuse through the pore solution. This motion would be very restricted if a continuous way of water does not exist. Previous studies [4] about gaseous water transport through concrete have shown that this liquid percolation continuous pathway usually exists for concrete in equilibrium with a relative humidity (RH) higher than about 70% [4]. It has been also suggested that the  $\text{Cl}^-$  diffusion coefficient should be negligible below a certain critical moisture content or critical RH of the same value [5]. It is reasonable that the  $\text{Cl}^-$  diffusion coefficient is strongly dependent on the RH of the atmosphere in equilibrium with concrete, especially for RH values close to 70%.

## 2. Experimental

### 2.1. Concretes tested

For this study, cylindrical concrete specimens, 20 cm in height and 10 cm in diameter, were cast following two mixes, whose dosages are shown in Table 1. These mixes were designed to provide target 28-day compressive strengths of 25 and 35 MPa, so they are designated as H-25 and H-35 following Ref. [6]. After casting, the specimens were compacted by vibration. They were cured, after demoulding, during 28 days in a fog room with an RH higher than 95% and at 20 °C. The raw materials were the following: two ordinary Portland cements with limestone (CEM II/A-L 32.5 for H-25 and CEM II/A-L 42.5 R for H-35), a limestone sand, two limestone gravels (4–6 and 6–12 mm, respectively), and distilled water. A water-reducing agent free of  $\text{Cl}^-$  (Plastiment HP-1, Sika) was used for mixing H-35. Table 1 also shows the mean compressive strengths obtained by testing six cylindrical

Table 1

Dosages and characteristics of the concretes tested

	Concrete	
	H-25	H-35
Dosage		
Cement ( $\text{kg/m}^3$ )	350.0	350.0
Sand ( $\text{kg/m}^3$ )	630.3	662.8
Gravel 4–6 mm ( $\text{kg/m}^3$ )	465.5	489.5
Gravel 6–12 mm ( $\text{kg/m}^3$ )	679.0	714.0
Plasticizer ( $\text{kg/m}^3$ )	–	1.4
w/c	0.6	0.5
Mean compressive strength (MPa)	27.9	40.8
Porosity (%)	16.3	12.7
Bulk specific gravity, dry ( $\text{g/cm}^3$ )	2.23	2.31

specimens (30 cm in height and 15 cm in diameter) and the porosities and bulk specific gravity (dry) measured through the hydrostatic balance method [7] for both concretes under study.

### 2.2. Water content control of samples

The concrete water contents selected for this work have been those in equilibrium with atmospheres of 54%, 75%, 86%, and >95% RH. The atmospheres of 54%, 75%, and 86% RH were obtained by means of saturated solutions of  $\text{Mg}(\text{NO}_3)_2 \cdot 6\text{H}_2\text{O}$ , NaCl, and KCl, respectively, kept in closed containers at 20 °C [8]. The specimens were pre-conditioned after curing and before exposure to the PVC combustion gases in the following ways: the specimens in equilibrium with an atmosphere of RH > 95% were kept in the curing chamber. The specimens in equilibrium with 86%, 75%, and 54% RH were dried during 1, 3, and 5 days, respectively, in a ventilated oven at 50 °C and after this, they were kept in the corresponding 86%, 75%, and 54% RH chambers for at least 3 weeks before testing. The attainment of equilibrium with the selected RH atmosphere was assured by checking the mass constancy of the specimens. This preconditioning with a drying step and an equilibration phase may be considered as essential in accordance with recommended procedures for obtaining a uniform distribution of the evaporable water in concrete specimens [9]. The degree of water saturation for each type of concrete and each humidity condition was measured by weighing representative samples with their natural water contents, just after removing them from their controlled humidity enclosures,  $m_h$ , after water saturation,  $m_s$ , and after oven drying at 105 °C,  $m_d$ .

$$\% \text{ water saturation} = \frac{m_h - m_d}{m_s - m_d} \times 100 \quad (1)$$

An important point to assure the validity of the experimental procedure is to check if the water content of the specimens is not altered during the exposure to PVC combustion gases. Therefore, the mass of the specimens was checked before and after these exposure experiments

and its variation was always equal or less than 1 g for 90% of the specimens and less than 3 g for the remaining 10%. Since the overall mass of the specimens is about 4 kg, the variation in water content due to these exposure tests may be considered negligible. After the exposure and during the diffusion period, the specimens were kept in their corresponding constant RH chambers.

Electrical resistivity measurements were performed with some of the specimens corresponding to the different concretes and atmospheres tested. The resistivity,  $\rho$ , was measured by using the positive feedback ohmic drop compensation facility of a potentiostat (Model 362, EG&G Instruments, Princeton NJ, USA).

### 2.3. Exposure of concrete specimens to PVC combustion gases

Once having finished the preconditioning step, the concrete specimens were submitted to interaction with PVC combustion gases without direct action of fire, following essentially an experimental procedure described previously [2]. An airtight plastic chamber with a vitrified ceramic hot plate was used for the thermal decomposition of portions of pure PVC resin. In these experiments, only the mould bases of the cylindrical specimens were exposed, the remaining faces were protected with insulating tape. In each run, four specimens were tested, and the quantity of PVC resin decomposed was adjusted to give a ratio between the mass of burnt PVC and the area of concrete surface exposed PVC/S of 40 mg PVC/cm<sup>2</sup> [2]. A few runs were performed with a lower PVC/S ratio of 10 mg/cm<sup>2</sup>. The duration of the exposure to PVC combustion gases was always an hour, after which the specimens were removed, weighed, and returned to their controlled humidity exposure conditions.

### 2.4. Diffusion tests program

The diffusion tests were performed by keeping the concrete specimens, after having been exposed to PVC combustion gases, during various storage periods at their controlled humidity conditions. The selected diffusion times were 1, 3, 10, 20, 60, and 180 days and 1 year. A number of specimens were kept for further tests at longer diffusion times. After completion of these storage periods, the specimens were removed and immediately submitted to a grinding process [10], to obtain powdered samples corresponding to thin successive parallel layers to the exposed surface of 1- or 2-mm thickness. The samples were analyzed for their acid-soluble chloride contents by a potentiometric titration procedure [11]. The Cl<sup>-</sup> concentrations have been corrected by subtracting the corresponding initial Cl<sup>-</sup> content of the concrete. The overall Cl<sup>-</sup> content in each concrete specimen was integrated from the measured concentration profile. This enabled the calculation of the relative chloride percentages (referred to overall ingressed Cl<sup>-</sup>) corresponding to

each sample constituting the profile. This way for expressing the chloride concentrations has been used in Figs. 2–5 in order to get a better assessment of the spatial distribution of Cl<sup>-</sup> within the specimens after interaction with PVC combustion gases.

## 3. Results

The mutual relationships among the water saturation degree of the concrete, calculated through Eq. (1), the electrical resistivity, and the RH of the atmosphere, are shown in Fig. 1. The water saturation percentage varies within the range from 30% to 80% for the concretes tested. It can be observed that for the same RH (54% and >95%), the degree of water saturation depends on the porosity of concrete: it is higher for the less porous concrete (H-35). The resistivity of concrete also shows a strong dependence on the equilibrium atmosphere RH and the degree of water saturation of concrete: it decreases about two orders of magnitude when the degree of water saturation increases from 30% to 70%, in good agreement with previous results [12,16].

Figs. 2–5 show the experimental Cl<sup>-</sup> concentration profiles corresponding to specimens of H-25 concrete in equilibrium with atmospheres of RH >95%, 86%, 75%, and 54%, respectively, submitted to the combustion gases of PVC with a PVC/S ratio of 40 mg/cm<sup>2</sup> and stored during periods from 1 day to about 1 year, in their corresponding controlled humidity enclosures. For the sake of clarity, not all the obtained profiles have been plotted in Figs. 2–5. Some preliminary results have been presented before [13]. From the profiles corresponding to a 1-day diffusion period, it is noticed that most of the Cl<sup>-</sup> in concretes subjected to the combustion gases of PVC presents in the outermost 3-mm layer of the specimens. This portion represents between 77% and 94% of total Cl<sup>-</sup> in these tests. This fact suggests that at the beginning of the transport process

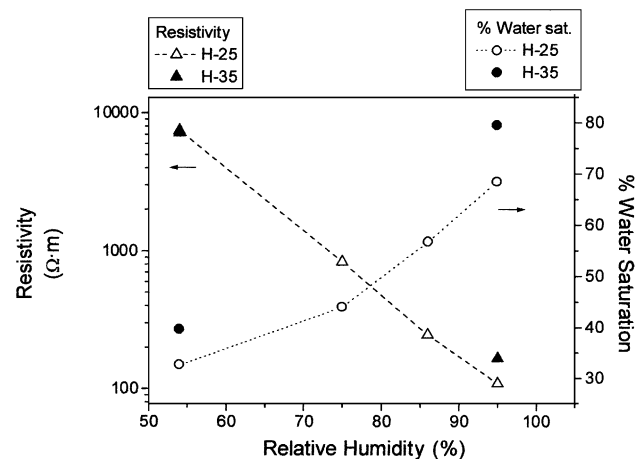


Fig. 1. Variation of the resistivity and the degree of water saturation with the RH of the equilibrium atmosphere for the concrete specimens tested.

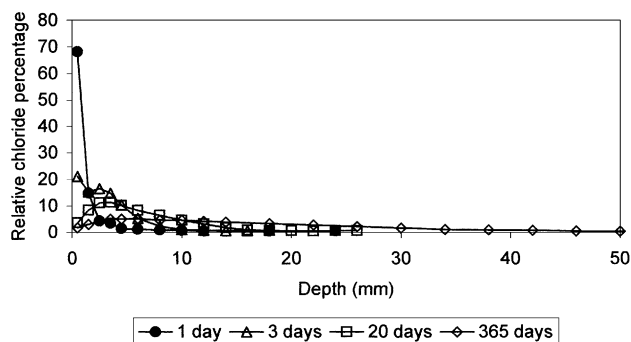


Fig. 2. Experimental  $\text{Cl}^-$  content profiles of H-25 concrete specimens in equilibrium with an atmosphere of  $\text{RH} > 95\%$ , submitted to interaction with PVC combustion gases with a PVC/S ratio of  $40 \text{ mg/cm}^2$ , after various times of diffusion.

practically all the diffusing substance is present at the surface. Therefore, the assumed initial conditions expressed in Eqs. (7) and (8) of Appendix A are adequately fulfilled. It is necessary to take into account that some  $\text{Cl}^-$  may have been transported from the surface inwards during 1 day of diffusion. The  $\text{Cl}^-$  content profiles corresponding to H-35 concrete specimens tested with a PVC/S ratio of  $40 \text{ mg/cm}^2$  and to H-25 specimens tested with a PVC/S ratio of  $10 \text{ mg/cm}^2$  (see Experimental section) are not shown here but are qualitatively similar to those plotted in Figs. 2–5.

The overall quantity of  $\text{Cl}^-$  laden in each concrete specimen,  $m_{\text{ex}}$ , has been integrated from the corresponding content profiles. Table 2 shows the mean amounts of  $\text{Cl}^-$  absorbed by the specimens tested under the same conditions, expressed in milligrams of  $\text{Cl}^-$  per square centimeter of exposed concrete surface. The amount of  $\text{Cl}^-$  absorbed shows some variability for each set of specimens, as indicated by the standard deviations in Table 2. These differences are due to the fact that not all the specimens included in each set have been tested in the same combustion run and to the difficulty in obtaining an homogeneous distribution of  $\text{HCl(g)}$  within the combustion chamber. Nevertheless, the mathematical treatment of each profile is independent of the rest, i.e., a single value of the diffusion

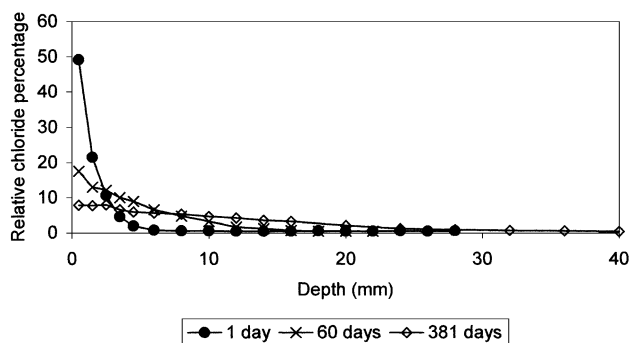


Fig. 3. Experimental  $\text{Cl}^-$  content profiles of H-25 concrete specimens in equilibrium with a  $86\% \text{ RH}$  atmosphere, submitted to interaction with PVC combustion gases with a PVC/S ratio of  $40 \text{ mg/cm}^2$ , after various times of diffusion.

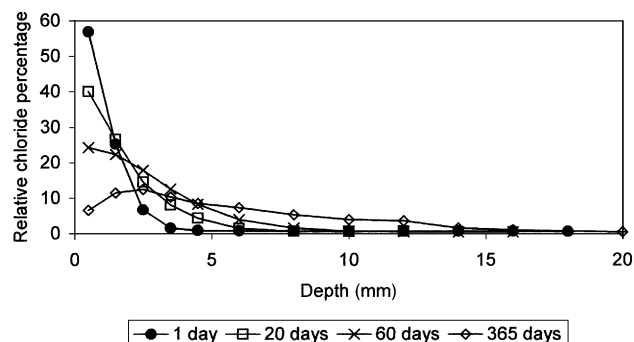


Fig. 4. Experimental  $\text{Cl}^-$  content profiles of H-25 concrete specimens in equilibrium with a  $75\% \text{ RH}$  atmosphere, submitted to interaction with PVC combustion gases with a PVC/S ratio of  $40 \text{ mg/cm}^2$ , after various times of diffusion.

coefficient is obtained from each profile (see Appendix A). Therefore, the variability found for the amount of absorbed  $\text{Cl}^-$  does not hinder either the validity of the procedure or the applicability of the model. The amount of  $\text{Cl}^-$  laden in each concrete specimen depends on the nature of concrete: the less porous concrete (H-35) absorbs less  $\text{Cl}^-$  under equality of the rest of conditions (see Table 2). The degree of water saturation does not show a clear influence trend upon the amount of  $\text{Cl}^-$  absorbed. Lastly, the relative  $\text{Cl}^-$  absorption, referred to the overall chlorine released by the burnt PVC samples, increases when the PVC/S ratio is decreased from 40 to  $10 \text{ mg PVC/cm}^2$ , in agreement with previous results [2].

## 4. Discussion

### 4.1. Shape and evolution of the chloride profiles

The  $\text{Cl}^-$  concentration profiles at 1 day of diffusion are shown in Figs. 2–5. It is appreciable from them that although most chloride deposited remains near the surface, low but detectable  $\text{Cl}^-$  concentrations may be found at maximum depths between 6 and 16 mm, in agreement with previous

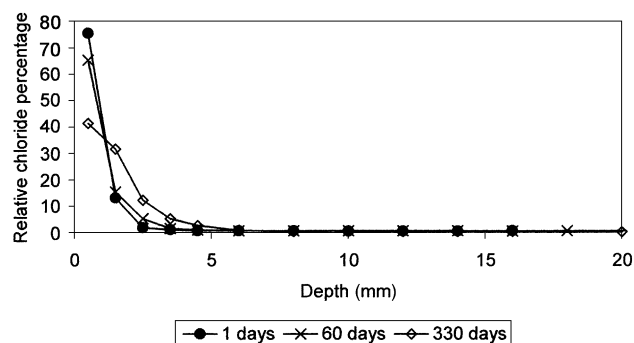


Fig. 5. Experimental  $\text{Cl}^-$  content profiles of H-25 concrete specimens in equilibrium with a  $54\% \text{ RH}$  atmosphere, submitted to interaction with PVC combustion gases with a PVC/S ratio of  $40 \text{ mg/cm}^2$ , after various times of diffusion.

Table 2  
Absorption of  $\text{Cl}^-$  by the concrete specimens tested

Concrete/ (PVC/S) ratio	Atmosphere RH (%)	Number of specimens	Mean $m_{\text{ex}}$ ( $\text{mg}/\text{cm}^2$ )	Standard deviation ( $\text{mg}/\text{cm}^2$ )	Mean relative $\text{Cl}^-$ absorption <sup>a</sup> (%)
H-25/40	>95	7	5.60	1.45	31.0
H-25/40	86	4	5.27	0.34	27.5
H-25/40	75	5	4.37	0.50	24.1
H-25/40	54	5	4.31	0.87	23.5
H-25/10	>95	4	2.63	0.44	44.6
H-35/40	>95	7	2.70	0.92	14.7
H-35/40	54	5	3.30	0.50	17.2

$m_{\text{ex}}$  is the amount of  $\text{Cl}^-$  absorbed per square centimeter of exposed surface. See Section 3 for details.

<sup>a</sup> The mean relative  $\text{Cl}^-$  absorptions refer to total chlorine released by the burnt PVC samples.

findings [2]. There is no clear influence of the concrete water content upon the shape of the profiles at 1 day of diffusion. On the other hand, the profiles at longer times confirm the expected strong influence of the degree of water saturation of the pore network of concrete upon the transport of  $\text{Cl}^-$ . The profiles corresponding to specimens in equilibrium with an atmosphere of RH >95% (Fig. 2) quickly develop an almost flat shape, indicating a rapid diffusion process. The profiles corresponding to specimens in equilibrium with 86% and 75% RH (Figs. 3 and 4) slowly change with time progressively and the profiles corresponding to 54% RH (Fig. 5) show only minor advance after 330 days of diffusion, indicating that the transport of  $\text{Cl}^-$  for this low concrete water content is very slow.

A  $\text{Cl}^-$  concentration maximum near the surface, at about 3–4 mm depth, is observed for the profiles corresponding to specimens in equilibrium with an RH > 95% atmosphere and for diffusion times longer than 10 days (see Fig. 2). It is also appreciable for specimens with a lower water content but for much longer diffusion times (Fig. 4). This maximum is not compatible with a pure diffusion process in a homogenous medium. Its presence may be explained, in principle, by the spatial heterogeneity of cast concrete specimens, which induces different transport properties in the concrete surface layers as compared with the bulk material [14,15]. Another explanation for the concentration maxima would be an alteration of the physical–chemical nature of the concrete surface layer due to the interaction with the gaseous hydrogen chloride released during the combustion of PVC. This may modify, for instance, the ability for  $\text{Cl}^-$  binding in a similar manner as is produced by carbonation of the surface layer.

#### 4.2. Application of the diffusion model

The particular solution to Fick's second law of diffusion corresponding to the instantaneous plane source case in a semi-infinite medium [3] is expressed in Eqs. (9) and (10) of Appendix A. The diffusion coefficient,  $D$ , and the total amount of diffusing substance,  $m$ , can be calculated by fitting the data of the experimental  $\text{Cl}^-$  concentration profiles to Eq. (10). This procedure allows one to check the consistency between calculated and measured param-

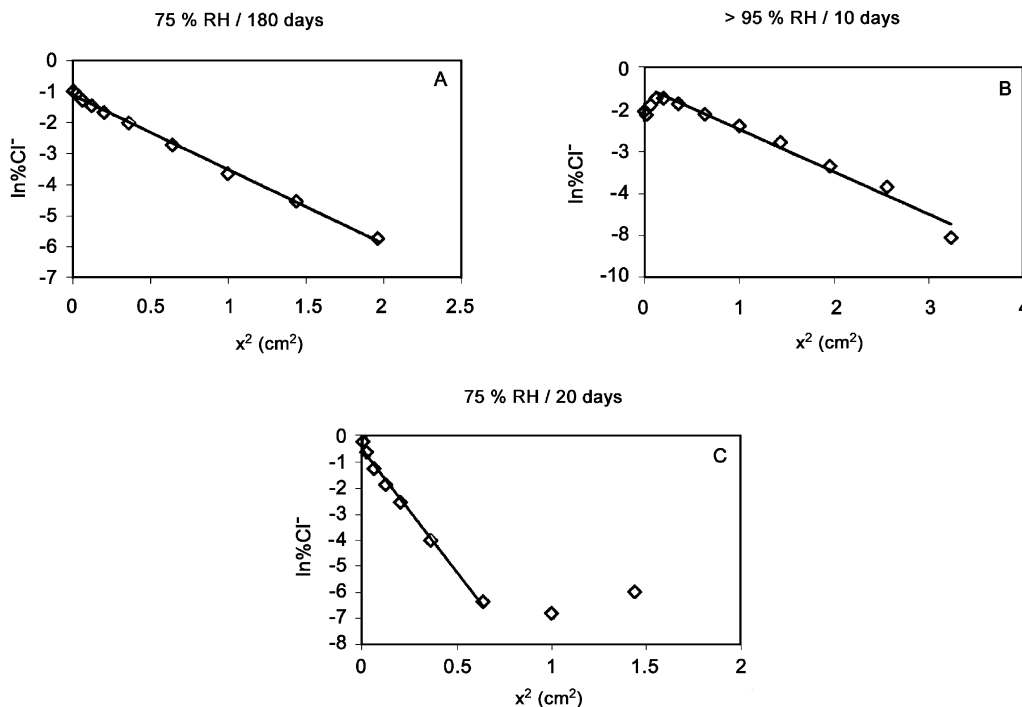


Fig. 6. Plots of  $\ln c$  versus  $x^2$  (see Appendix A). The data correspond to H-25 concrete specimens, submitted to interaction with PVC combustion gases with a PVC/S ratio of 40  $\text{mg}/\text{cm}^2$  and after various times of diffusion. Points: experimental data. Lines: best fit straight lines following Eq. (10), corresponding to the selected set of points (see Section 4.2).

ters, by comparing the derived value of  $m$  with the experimental total amount of absorbed  $\text{Cl}^-$ ,  $m_{\text{ex}}$  (see Section 3).

When plotting the values of  $\ln c$  versus  $x^2$  for the profiles obtained, following Eq. (10), we have found three kinds of behaviour that have been depicted in Fig. 6: some plots show an almost perfect linear trend (Fig. 6A), a few plots show low values of  $\ln c$  for the samples obtained near the surface of the specimen, giving rise to a small branch with positive slope (Fig. 6B), and lastly, some plots show two different linear branches, one with negative slope and the second almost horizontal (Fig. 6C). The deviation from linearity shown in Fig. 6B is always associated with the presence of maxima in the measured pro-

files (see Section 4.1). Since these maxima are likely to be due to natural and/or induced heterogeneity of concrete, the few points constituting the small branch with positive slope in Fig. 6B have not been considered for the fittings to Eq. (10), in a similar way as is done when fitting the data of a concrete chloride profile to the standard error function solution of Fick's second law.

The behaviour depicted in Fig. 6C is observed for specimens in equilibrium with all the studied humidities (see Table 3), but in the case of the concrete with the highest moisture content ( $\text{RH} > 95\%$ ), this type of deviation appears mainly for the specimens tested after short diffusion times. For the concrete in equilibrium with a 54% RH atmosphere,

Table 3  
Results of the fitting of the experimental  $\text{Cl}^-$  profiles to Eq. (10)

Concrete/(PVC/S) ratio ( $\text{mg}/\text{cm}^2$ )	Atmosphere RH (%)	Diffusion time (days)	Diffusion coefficient, $D$ ( $\text{m}^2/\text{s}$ ) $\times 10^{-12}$	$m/m_{\text{ex}}$	Linear regression correlation coefficient, $r$	Estimated diffusion coefficient ( $\text{m}^2/\text{s}$ ) $\times 10^{-12}$
H-25/40	>95	1 <sup>a</sup>	15.6	0.65	0.916	<b>3.84</b>
H-25/40	>95	3 <sup>a</sup>	34.8	0.89	0.987	
H-25/40	>95	10	14.2	1.50	0.990	
H-25/40	>95	20 <sup>a</sup>	13.5	1.15	0.998	
H-25/40	>95	60	<b>2.89</b>	1.07	0.960	
H-25/40	>95	180	<b>3.73</b>	1.03	0.973	
H-25/40	>95	365 <sup>a</sup>	<b>4.90</b>	1.02	0.999	<b>2.68</b>
H-25/40	86	1 <sup>a</sup>	22.0	0.81	0.979	
H-25/40	86	60 <sup>a</sup>	<b>3.08</b>	0.99	0.997	
H-25/40	86	180	<b>2.07</b>	1.08	0.974	
H-25/40	86	381 <sup>a</sup>	<b>2.90</b>	1.09	0.995	<b>1.01</b>
H-25/40	75	1 <sup>a</sup>	10.5	0.82	0.985	
H-25/40	75	20 <sup>a</sup>	<b>1.53</b>	0.90	0.996	
H-25/40	75	60	<b>1.17</b>	0.92	0.987	
H-25/40	75	180	<b>0.67</b>	0.99	0.999	
H-25/40	75	365 <sup>a</sup>	<b>0.66</b>	1.06	0.988	
H-25/40	54	1 <sup>a</sup>	10.6	0.49	0.927	<b>0.077</b>
H-25/40	54	20 <sup>a</sup>	0.68	0.66	0.981	
H-25/40	54	60 <sup>a</sup>	0.33	0.48	0.909	
H-25/40	54	180	<b>0.077</b>	0.90	0.989	
H-25/40	54	330 <sup>a</sup>	0.069	0.89	0.988	
H-35/40	>95	1 <sup>a</sup>	26.1	0.68	0.923	<b>6.05</b>
H-35/40	>95	3 <sup>a</sup>	13.0	0.84	0.980	
H-35/40	>95	10 <sup>a</sup>	<b>7.99</b>	0.97	0.991	
H-35/40	>95	20 <sup>a</sup>	<b>8.61</b>	1.06	0.998	
H-35/40	>95	60	<b>4.44</b>	1.00	0.947	
H-35/40	>95	180 <sup>a</sup>	<b>3.17</b>	1.06	0.999	
H-35/40	>95	365 <sup>a</sup>	3.18	0.81	0.993	<b>0.071</b>
H-35/40	54	1 <sup>a</sup>	8.35	0.70	0.954	
H-35/40	54	20 <sup>a</sup>	0.94	0.52	0.922	
H-35/40	54	60 <sup>a</sup>	0.16	0.72	0.944	
H-35/40	54	180 <sup>a</sup>	0.22	0.50	0.951	
H-35/40	54	365 <sup>a</sup>	<b>0.071</b>	0.90	0.988	<b>4.00</b>
H-25/10	>95	1 <sup>a</sup>	27.7	0.75	0.942	
H-25/10	>95	60	11.2	1.19	0.995	
H-25/10	>95	180	<b>4.00</b>	1.05	0.961	
H-25/10	>95	365 <sup>a</sup>	4.44	1.15	0.997	

<sup>a</sup> The cases for which the experimental points constituting the horizontal branch of the plot have not been considered for the fitting to Eq. (10). See Section 4.2 for details.

the behaviour of Fig. 6C is observed almost for all specimens. The fitting of all data of the profiles type (Fig. 6C) to Eq. (10) systematically yielded values of  $D$  higher than those obtained with the rest of the profiles. This fact was paralleled with the obtainment of calculated amounts of ingressed  $\text{Cl}^-$ ,  $m$ , lower than the experimentally measured values,  $m_{\text{ex}}$ . By examination of Fig. 6C and Eq. (10), it may be appreciated that the low but detectable  $\text{Cl}^-$  concentrations found at depths higher than 8 mm, which are similar to those found at the 1-day diffusion profile (Fig. 4), induce a decrease of the absolute value of the calculated slope and a decrease of the calculated intercept, and hence an increase of the derived  $D$  and a decrease of the derived  $m$ . The presence of the two branches in Fig. 6C suggests the contribution of another rather quick transport process of  $\text{Cl}^-$ , giving rise to the unexpectedly high  $\text{Cl}^-$  concentrations at depths higher than 8 mm. It must be taken into account that the measured  $\text{Cl}^-$  contents in the horizontal branch region of Fig. 6C should have been below the detection limit if the slope would have been the same as

the negative slope branch. This effect may be explained, in principle, by a quick transport of  $\text{Cl}^-$  during the exposure to the combustion gases of PVC: the gaseous hydrogen chloride may penetrate easily by diffusion in gas phase through the nonsaturated pore network, thus contributing to an early ingress of  $\text{Cl}^-$  at high depths. This effect would be more important for the profiles obtained at short diffusion times. Nevertheless, the possible influence of small errors in the determination of net  $\text{Cl}^-$  concentrations in the region of the horizontal branch cannot be ruled out, for the plots like Fig. 6C. Taking into account this discussion, it was decided to disregard the points corresponding to the horizontal branch in the plots similar to Fig. 6C for the fitting to Eq. (10). The cases for which these points have not been considered are indicated by superscript a in Table 3. In all cases, the elimination of these points for the fitting has led to a better agreement between  $m$  and  $m_{\text{ex}}$ .

Table 3 shows the results of the fitting of all the obtained  $\text{Cl}^-$  profiles to Eq. (10), taking into account all the particular situations discussed in the preceding paragraphs.

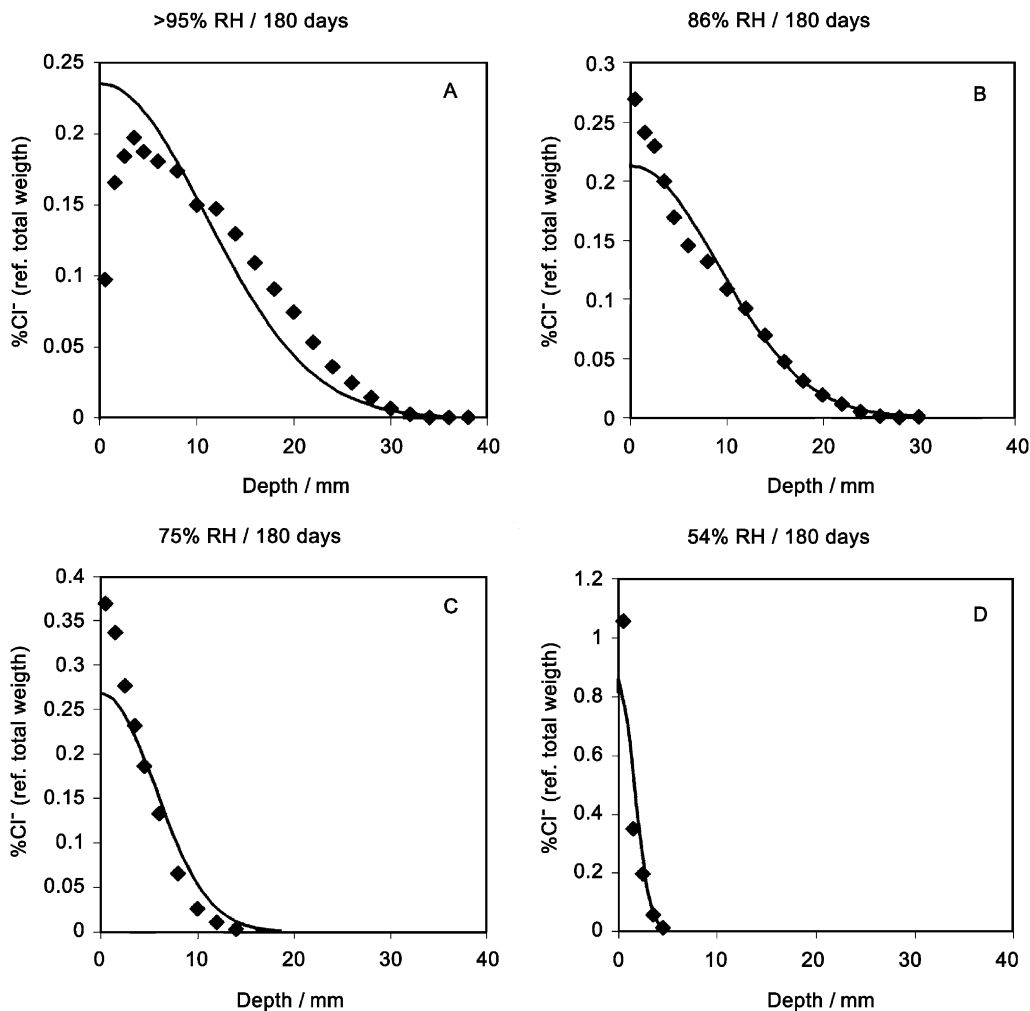


Fig. 7. Experimental (points) and calculated (lines)  $\text{Cl}^-$  content profiles of H-25 concrete specimens in equilibrium with different RH atmospheres, submitted to interaction with PVC combustion gases with a PVC/S ratio of 40 mg/cm<sup>2</sup> and after 180 days of diffusion (see Section 4.2).

An evolution with time of the derived parameters is appreciable:  $D$  is generally higher at short diffusion times and decreases to reach an almost constant value for longer times, while the quotient  $m/m_{\text{ex}}$  is low at short diffusion times and increases to reach values near unity at longer times. This evolution is slower for the specimens in equilibrium with a 54% RH atmosphere. The origin of this evolution may be explained, in principle, by the coexistence of two mechanisms of  $\text{Cl}^-$  transport, as discussed in the preceding paragraph. The fact of having eliminated the points constituting a visually apparent horizontal branch in the plots type (Fig. 6C) does not avoid the interference of the quick transport mechanism of  $\text{Cl}^-$  upon the rest of the points. This interference is progressively less important as the diffusion of  $\text{Cl}^-$  in liquid phase develops, except for the specimens in equilibrium with a 54% RH atmosphere. For these latter cases, the slowness of the  $\text{Cl}^-$  diffusion in the liquid phase maintains a situation in which the interference of this quick early transport is notorious even at longer diffusion times. The value of the quotient  $m/m_{\text{ex}}$  provides a guidance to assess when this interference may be considered negligible. In this work, it has been adopted as pass criterion for  $m/m_{\text{ex}}$  the range of values between 0.90 and 1.10, this range implies an acceptable bias of  $\pm 10\%$ . It may be observed that when  $m/m_{\text{ex}}$  reaches values within the 0.90–1.10 range, the values of  $D$  are approximately constant and the linear regression coefficient of the plot is equal or higher than .95, indicating a good fitting of the data to Eq. (10). Therefore, the final estimated value of  $D$  for each set of experimental conditions (seventh column in Table 3) has been calculated as the mean of  $D$  values corresponding to cases passing the  $m/m_{\text{ex}}$  criterion. These latter values are highlighted in bold characters in Table 3.

Fig. 7 shows the experimental and calculated  $\text{Cl}^-$  content profiles corresponding to H-25 concrete specimens in equilibrium with all the humidities, tested after 180 days. The calculated profiles have been obtained by applying Eq. (9), with the corresponding estimated value of  $D$  (seventh column of Table 3) and the corresponding experimental amount of absorbed  $\text{Cl}^-$ ,  $m_{\text{ex}}$ . A good concordance between experimental and calculated profiles is apparent from Fig. 7, giving some degree of support to the model used in this work. A difference between experimental and calculated  $\text{Cl}^-$  concentrations is observed in Fig. 7A at low depths from the surface. This fact is related to the presence of the maxima in the experimental profiles (see Section 4.1).

#### 4.3. Dependence of the chloride diffusion coefficient on the studied variables

The estimated  $\text{Cl}^-$  diffusion coefficient shows a strong dependence on the degree of water saturation of concrete (Fig. 8A).  $D$  decreases about two orders of magnitude when the percentage of water saturation diminishes from 70% to 30% approximately. The variation of  $D$  is not high in the range between 70% and 45% of water saturation, having

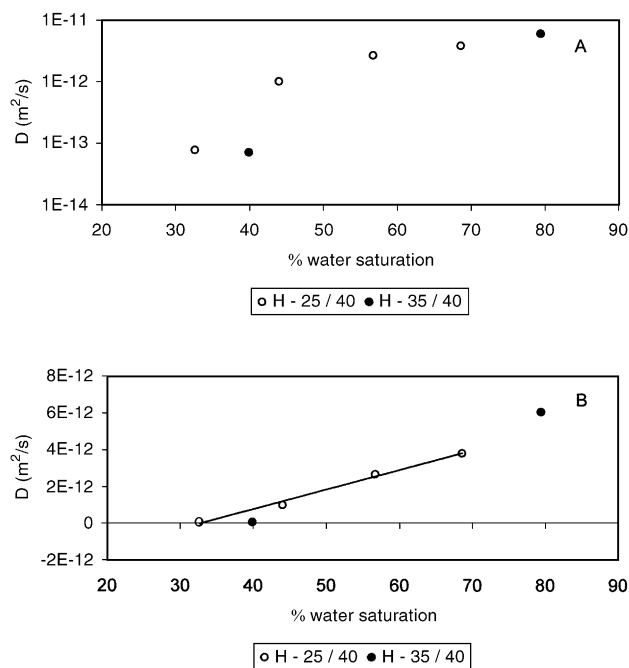


Fig. 8. Relationship between the obtained  $\text{Cl}^-$  diffusion coefficients and the degree of water saturation of the specimens tested.  $\circ$ ,  $\bullet$ : PVC/S=40  $\text{mg}/\text{cm}^2$ .

obtained values between  $4 \times 10^{-12}$  and  $1 \times 10^{-12}$   $\text{m}^2/\text{s}$  (see also Table 3). For lower degrees of water saturation, the decrease of  $D$  becomes very important, and values below  $1 \times 10^{-13}$   $\text{m}^2/\text{s}$  may be reached for concrete specimens with percentages of water saturation between 30% and 40%, imposed by equilibrium with a 54% RH atmosphere. The data corresponding to H-25 specimens, tested with a PVC/S ratio of 40  $\text{mg}/\text{cm}^2$ , have been linearly fit by a least squares method (Fig. 8B). The best fit ( $r=.996$ ), has been obtained with Eq. (2):

$$D = 1.068 \times 10^{-13} S - 3.496 \times 10^{-12} \quad (2)$$

where  $D$  is expressed in  $\text{m}^2/\text{s}$  and  $S$  is the percentage of water saturation. Eq. (2) is totally empiric and is intended to describe only the variation of the chloride diffusion coefficient for concrete H-25, within the range of degrees of water saturation between 33% and 69%.

The variation of  $D$  with the degree of water saturation and hence with the RH of the equilibrium atmosphere may be considered as expected. For degrees of water saturation below about 45%, i.e., RH of the atmosphere below 75%, the  $\text{Cl}^-$  diffusion coefficient value drops to values in the order of  $7 \times 10^{-14}$   $\text{m}^2/\text{s}$ . This is due to the likely discontinuity of the aqueous phase within the pore network of concrete in equilibrium with atmospheres of  $\text{RH} < 70\%$  [4,16]. Nevertheless, it should be considered the practically unchanged  $\text{Cl}^-$  content profile shape, after 1 year of diffusion (Fig. 5), for the specimens in equilibrium with a 54% RH. This low degree of evolution of the diffusion process implies a lower confidence on the calculated  $D$

values, even at 1 year, since the linear regression plots have a low number of points. An extension of the diffusion testing times would be desirable for these low-water-content specimens.

It is interesting to look at the effect of changing the nature of concrete from H-25 to H-35. Table 3 shows that for the two RH tested (>95% and 54%),  $D$  is very similar for both concretes. For RH >95%, the final estimated value of  $D$  for H-35 is slightly higher than that for H-25, but looking at the whole result sets for both concretes, it is apparent that both sets tend to converge to a very similar value of  $D$ . This fact is somewhat surprising taking into account that H-35 is less porous than H-25 (see Table 1). Fig. 1 shows that for the same RH, the degree of water saturation is higher for H-35 than for H-25. It is likely that, for the same RH, the liquid phase within the pore network of H-35 is more continuous than that of H-25 due to the higher relative moisture content of the former concrete, and hence the diffusion of  $\text{Cl}^-$  would be facilitated. This situation would eventually counterbalance the opposite effect of the higher porosity (better connectivity between pores and lower tortuosity) of H-25. The net influence of porosity would be probably better assessed by comparing data obtained at the same degree of water saturation, not at the same RH. The higher degree of water saturation of the less porous concrete for the same RH may be explained by a different distribution of pore diameters between H-35 and H-25. Taking into account that the former concrete was prepared with a lower w/c ratio (see Table 1), it is likely that H-35 has a larger proportion of pores with small diameters than H-25 [16]. When a partially moist porous solid interacts with an atmosphere with a given RH to reach the hygric equilibrium, liquid water tends to condense by capillarity in the pores with radius below a given value,  $R$ . On the other hand, the pores with radius larger than  $R$  tend to be emptied due to evaporation [4]. This behaviour is approximately described by the Kelvin–Laplace equation [4]. Nevertheless, the results presented in this work do not allow one to confirm these hypothetical considerations. Further applications of the proposed experimental approach and model to concretes with different pore

structures are needed to ascertain the influence of porosity on the  $\text{Cl}^-$  diffusion coefficient under nonsaturated conditions.

The effect of changing the PVC/S ratio from 40 to 10  $\text{mg}/\text{cm}^2$ , is practically negligible since the estimated  $D$  values are practically equal for both PVC/S ratios, at least for the RH >95% equilibrated specimens tested here (see Table 3). This fact is as expected since changing the PVC/S ratio in a wide range has been shown before not to modify sensibly the qualitative shape of the  $\text{Cl}^-$  content profiles of different concretes submitted to exposure to PVC combustion gases [2].

Fig. 9 shows the almost inverse relationship found between the chloride diffusion coefficient and the resistivity for the concrete specimens with well-characterized moisture contents used in this work. This may be explained by considering that for nonsaturated concrete,  $\rho$  is mainly dependent on the relative amount of moisture and its distribution within the concrete pore network [16], which in turn determines the kinetics of ionic diffusion through the material. All data in Fig. 9 have been adjusted by a least squares method to a potential function ( $D = a\rho^b$ ). The best fit ( $r = .985$ ) has been obtained with Eq. (3):

$$D = 6.026 \times 10^{-10} \times \rho^{-0.9997}. \quad (3)$$

The same mathematical dependence between  $D$  and  $\rho$  has been theoretically predicted [17,18] and experimentally confirmed [19] for water-saturated concretes. This relationship, now extended to nonsaturated conditions, may be considered as a support to the proposal of using the resistivity test to universally characterize mass transport processes in concrete [17,18]. It is interesting to note that the numerical value obtained for the constant  $6.026 \times 10^{-10} \Omega \text{ m}^3/\text{s}$  is in fairly good agreement with those that may be derived [18] or have been obtained [19] for saturated concretes, taking into account the different approaches used.

The test method and model described in this work allow one to obtain experimental values of the chloride diffusion coefficient through nonsaturated concrete. The results presented may not be considered as definitive mainly in view of the time dependence of the derived values of  $D$  and the low degree of development of the diffusion process for concrete in equilibrium with a low RH atmosphere. The comparison between the calculated and experimentally determined total amounts of diffusing substance (see Section 4.2) provides a consistency check for selecting the results that may be considered as most reliable. The time needed for obtaining consistent values of  $D$  for concrete equilibrated with atmospheres of RH >75% is of about 60 days (see Table 3). This period is similar to that required for natural diffusion through saturated concrete (ponding tests). For specimens in equilibrium with low RH atmospheres, the testing time should be about 1 year or longer. The dependence of the determined values of  $D$  on the degree of water saturation (Fig. 8) is in agreement with the qualitative prediction of an almost negligible value of  $D$  for RH of the equilibrium

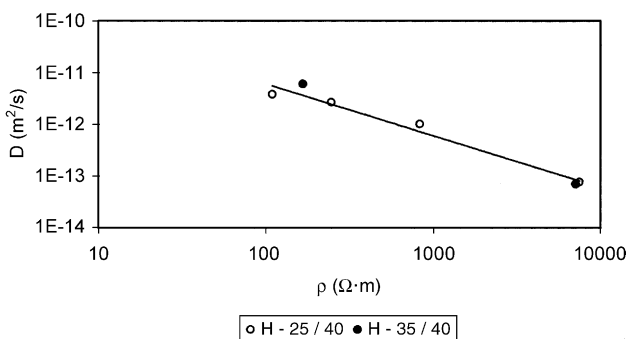


Fig. 9. Relationship between the obtained  $\text{Cl}^-$  diffusion coefficients and the resistivity of the specimens tested. ○, ●: PVC/S=40  $\text{mg}/\text{cm}^2$ .

atmosphere lower than 70% [5]. Nevertheless, the lack of alternative experimental approaches and quantitative theoretical methods of calculation of  $D$  under nonsaturated conditions prevents the checking of the validity of the proposed procedure. More research is in progress in order to obtain results at longer diffusion times, with different concrete compositions, and also to account for the chloride binding ability of concrete.

## 5. Conclusions

An experimental test method has been designed to measure the diffusion coefficient of chloride ions through nonsaturated concretes with controlled water contents. The obtained diffusion coefficients decrease about two orders of magnitude when the percentage of water saturation of concrete diminishes from 80% to 30% approximately. Nevertheless, this decrease is more important for water saturation lower than 45%. Values of  $D$  below  $1 \times 10^{-13} \text{ m}^2/\text{s}$  may be reached for concrete specimens in equilibrium with a 54% RH atmosphere. The electrical resistivity of the concrete specimens with well-characterized moisture contents appears to be a good indicator for assessing the diffusion properties of chloride ions through nonsaturated concrete.

## Acknowledgments

This work has been financially supported by the Conselleria d'Educació i Ciència de la Generalitat Valenciana through project GV-3224/95 and grant GR00-24, and by the Ministerio de Ciencia y Tecnología of Spain through project BQU2001-0837-C02-01. We also thank Compañía Valenciana de Cementos Portland (Sant Vicent del Raspeig, Alacant), Pavasal (Alacant), and Hispavic Industrial (Solvay) for donating the cements, aggregates, and PVC resin, respectively.

## Appendix A. Solution to Fick's second law of diffusion for the instantaneous plane source case

Fick's second law describes planar diffusion through the  $x$ -axis:

$$\frac{\partial c}{\partial t} = D \frac{\partial^2 c}{\partial x^2} \quad (4)$$

with  $D$  ( $\text{m}^2/\text{s}$ ) as the diffusion coefficient. Applying appropriate initial conditions, Eq. (4) can be solved to obtain the diffusing substance concentration  $c$  as a function of time  $t$  and position  $x$ .

For the case of instantaneous plane source in a semi-infinite media, we assume that the total amount of diffusing substance  $m$  is initially deposited on the semi-infinite media

surface and no other source of diffusing substance is present throughout the diffusion process. Therefore, initial conditions are as follows [3]:

1. The total amount of diffusing substance is constant

$$m = \int_0^\infty c dx \geq 0 \quad (5)$$

2. Far enough from the surface, there is no diffusing substance:

$$c = 0 \text{ for } x = \infty \text{ and } t \geq 0 \quad (6)$$

3. Initially all the diffusing substance remains on the surface:

$$c = 0 \text{ for } x > 0 \text{ and } t = 0, \quad (7)$$

$$c = \infty \text{ for } x = 0 \text{ and } t = 0, \quad (8)$$

Solving Eq. (4) with conditions (5), (6), (7) and (8) yields the following expression [3]:

$$c = \frac{m}{\sqrt{\pi D t}} \exp\left(-\frac{x^2}{4 D t}\right). \quad (9)$$

Eq. (9) can be linearized by taking logarithms:

$$\ln c = \ln \frac{m}{\sqrt{\pi D t}} - \frac{x^2}{4 D t}. \quad (10)$$

Experimental data can be fitted to Eq. (10). Linear regression of  $\ln c$  versus  $x^2$  yields slope  $-1/(4 D t)$  and intercept  $\ln(m/\sqrt{\pi D t})$  from which we can obtain the diffusion coefficient  $D$  and the total amount of diffusing substance  $m$ .

## References

- [1] S. Chatterji, On the non-applicability of unmodified Fick's law to ion transport through cement based materials, in: L.O. Nilsson, J.P. Ollivier (Eds.), Proceedings of the 1st International Workshop on Chloride Penetration Into Concrete, RILEM Publications, Cachan, France, 1997, pp. 64–73.
- [2] M.A. Climent, E. Viqueira, G. de Vera, M.M. López, Chloride contamination of concrete by interaction with PVC combustion gases, *Cem. Concr. Res.* 28 (1998) 209–219.
- [3] J. Crank, *The Mathematics of Diffusion*, second ed., Oxford Univ. Press, Oxford, UK, 1975, pp. 11–13.
- [4] M. Buil, J.P. Ollivier, Conception des bétons: La structure poreuse, in: J. Baron, J.P. Ollivier (Eds.), *La Durabilité des Bétons*, Presses de l'École Nationale de Ponts et Chaussées, Paris, 1992, pp. 63–81.
- [5] L.O. Nilsson, A numerical model for combined diffusion and convection of chloride ion in non-saturated concrete, in: C. Andrade, J. Kropp (Eds.), Proceedings of the 2nd International Workshop on Testing and Modeling the Chloride Ingress Into Concrete, RILEM Publications, Cachan, France, 2000, pp. 261–275.

- [6] Instrucción de Hormigón Estructural (EHE), Ministerio de Fomento, Madrid, Spain, 1998.
- [7] ASTM C 642-90, Standard Test Method for Specific Gravity, Absorption and Voids in Hardened Concrete, American Society for Testing and Materials, Philadelphia, USA, 1994.
- [8] DIN 50008: Part 1. Standard Atmospheres Over Aqueous Solutions, Deutsches Institut für Normung (DIN), Berlin, Germany, 1981.
- [9] RILEM TC 116-PCD, Permeability of concrete as a criterion of its durability, preconditioning of concrete test specimens for the measurement of gas permeability and capillary absorption of water, *Mater. Struct.* 32 (1999) 174–179.
- [10] Profile Grinder (PF-1100), Germann Instruments, Copenhagen, Denmark, 1996.
- [11] M.A. Climent, E. Viqueira, G. de Vera, M.M. López, Analysis of acid-soluble chloride in cement, mortar and concrete by potentiometric titration without filtration steps, *Cem. Concr. Res.* 29 (1999) 893–898.
- [12] W. López, J.A. González, Influence of the degree of pore saturation on the resistivity of concrete and the corrosion rate of steel reinforcement, *Cem. Concr. Res.* 23 (1993) 368–376.
- [13] M.A. Climent, G. de Vera, J.F. López, C. García, C. Andrade, Transport of chlorides through non-saturated concrete after an initial limited chloride supply, in: C. Andrade, J. Kropp (Eds.), *Proceedings of the 2nd International Workshop on Testing and Modeling the Chloride Ingress Into Concrete*, RILEM Publications, Cachan, France, 2000, pp. 173–187.
- [14] C. Andrade, J.M. Díez, C. Alonso, Modeling of skin effects on diffusion processes in concrete, in: L.O. Nilsson, J.P. Ollivier (Eds.), *Proceedings of the 1st International Workshop on Chloride Penetration Into Concrete*, RILEM Publications, Cachan, France, 1997, pp. 182–191.
- [15] D.P. Bentz, X. Feng, R.D. Hooton, Time dependent diffusivities: Possible misinterpretation due to spatial dependence, in: C. Andrade, J. Kropp (Eds.), *Proceedings of the 2nd International Workshop on Testing and Modeling the Chloride Ingress Into Concrete*, RILEM Publications, Cachan, France, 2000, pp. 225–233.
- [16] D. Burchler, B. Elsener, H. Böhni, Electrical resistivity and dielectric properties of hardened cement paste and mortar, in: C.L. Page, P.B. Bamforth, J.W. Figg (Eds.), *Proceedings of the 4th International Symposium on Corrosion of Reinforcement in Concrete Construction*, Royal Society of Chemistry, Cambridge, UK, 1996, pp. 283–293.
- [17] C. Andrade, C. Alonso, S. Goñi, Possibilities for electrical resistivity to universally characterize mass transport processes in concrete, R.K. Dhir, M.R. Jones (Eds.), *Proceedings of the Concrete 2000 Conference*, vol. 2, E & FN Spon, London, 1993, pp. 1639–1652.
- [18] C. Andrade, M.A. Sanjuán, A. Recuero, O. Río, Calculation of chloride diffusivity in concrete from migration experiments in non steady-state conditions, *Cem. Concr. Res.* 24 (1994) 1214–1228.
- [19] R.B. Polder, Chloride diffusion and resistivity testing of five concrete mixes for marine environment, in: L.O. Nilsson, J.P. Ollivier (Eds.), *Proceedings of the 1st International Workshop on Chloride Penetration Into Concrete*, RILEM Publications, Cachan, France, 1997, pp. 225–233.